

## Vortex avalanches with robust statistics observed in superconducting niobium

E. Altshuler,<sup>1,2</sup> T. H. Johansen,<sup>2,3</sup> Y. Paltiel,<sup>4</sup> Peng Jin,<sup>2</sup> K. E. Bassler,<sup>5</sup> O. Ramos,<sup>1</sup> Q. Y. Chen,<sup>2</sup> G. F. Reiter,<sup>5</sup> E. Zeldov,<sup>4</sup> and C. W. Chu<sup>2,5,6,7</sup>

<sup>1</sup>*Superconductivity Laboratory, IMRE-Physics Faculty, University of Havana, 10400 Havana, Cuba*

<sup>2</sup>*Texas Center for Superconductivity, University of Houston, Houston, Texas 77204-5002, USA*

<sup>3</sup>*Department of Physics, University of Oslo, P.O. Box 1048 Blindern, N-0316 Oslo, Norway*

<sup>4</sup>*Condensed Matter Physics Department, Weizmann Institute of Science, Rehovot 76100, Israel*

<sup>5</sup>*Department of Physics, University of Houston, Houston, Texas 77204-5005, USA*

<sup>6</sup>*Lawrence Berkeley National Laboratory, Berkeley, California 94720, USA*

<sup>7</sup>*Hong Kong University of Science and Technology, Clear Water Bay, Kowloon, Hong Kong*

(Received 3 June 2004; published 11 October 2004)

By combining micro-Hall probe and magneto-optical imaging techniques we have been able to examine vortex avalanches at different locations of the ridgelike magnetic topography of superconducting niobium samples as the external field is slowly increased. The avalanche size distributions are shown to be power laws for two decades with very similar critical exponents at all locations, thus demonstrating a remarkable robustness in the details of the flux penetration dynamics.

DOI: 10.1103/PhysRevB.70.140505

PACS number(s): 74.25.Qt, 05.65.+b, 45.70.Ht

Avalanche dynamics is observed in many physical systems ranging from sandpiles to superconductors.<sup>1,2</sup> While the experimental evidence of their existence is beyond doubt, the nature and robustness of the resulting avalanche size distributions has been a subject of intense debate, mainly due to the fact that they are central to the theory of self-organized criticality (SOC),<sup>3</sup> and also to more recent theories, such as avalanches driven by coherent noise (ADCN).<sup>4</sup> SOC occurs when a slowly driven system “organizes” itself into a marginally stable stationary state through scale-invariant avalanches which have a power-law size distribution  $P(s) \sim s^{-\tau}$ , where the value of the critical exponent  $\tau$  is universal in the sense that it should be robust to changes in the system.

DeGennes suggested as early as 1966 that avalanche dynamics could be present in the superconducting critical state.<sup>5</sup> When an external magnetic field is raised above a certain critical value, a type II superconductor becomes a host for quantized magnetic vortices, which nucleate at the edges and are driven inwards by their mutual repulsion. In most materials this motion is impeded by microscopic defects acting as “pinning sites,” with the result that the vortices pile up with a characteristic density gradient, producing the marginally stable “critical state.”<sup>6</sup> This, plus the fact that the motion of superconducting vortices is overdamped led Tang<sup>7</sup> to propose that SOC may exist in type-II superconductors, and prompted others to turn to type-II superconductors to test SOC ideas.

Field and co-workers’ experiments,<sup>8</sup> and similar ones performed by Heiden and Rochlin,<sup>9</sup> detected vortex avalanches by means of large pick-up coils in the center of Pb-In and Nb-Ti cylinders. The former authors found power-law distributions of avalanche sizes, which were interpreted as a clear indication of SOC, but there are two important drawbacks in this setup. First, the actual number of flux lines involved in each avalanche is very difficult to estimate. Second, only the avalanches leaving the superconductor are measured, which poses an extra difficulty to compare with SOC theory.

Direct observation of avalanche dynamics with single vortex resolution is today possible using micro-Hall probes. With this technique Seidler *et al.*<sup>10</sup> found that avalanchelike behavior occurs at high fields and very low temperatures in YBaCuO crystals. The avalanche statistics, later worked out in Ref. 11, was quite limited, being based on only a few hundred events. Nowak *et al.*<sup>12</sup> studied niobium thin films where the statistics was improved, although avalanche sizes below 50 vortices were absent. As pointed out by the authors, such films exhibit a thermomagnetic instability, or catastrophic flux jumps, which may camouflage other basic dynamical features. This is coherent with the results by Esquinazi *et al.* in thin Nb films.<sup>13</sup> Recently, much thicker niobium samples were investigated by Behnia *et al.*,<sup>14</sup> who found only very small avalanches under the Hall probe area, leaving an open question whether the distribution is a power-law or stretched exponential.

Local avalanche measurements can be improved by first mapping out the global magnetic landscape in which the Hall probes are placed. Therefore, we made magneto-optical (MO) imaging of the flux penetration in our superconducting sample, a Nb foil of dimensions  $1.5 \times 1.5 \times 0.25$  mm<sup>3</sup>, and carefully superimposed such images onto a picture taken afterwards of the Hall probe array attached to the large face of the sample. The MO pictures are obtained using a Faraday-active ferrite garnet film mounted on top of the superconductor, which is viewed through crossed polarizers in a microscope. We choose to study Nb because it has been the type-II superconductor most used in avalanche dynamics measurements in recent years,<sup>12–14</sup> and because the values of its relevant superconducting parameters show a remarkable repeatability from sample to sample, and from author to author [ $T_c \approx 9$  K,  $H_{c1}(4.2$  K)  $\approx 300$  Oe,  $H_{c2}(4.2$  K)  $\approx 4000$  Oe]. Figure 1 shows the MO image recorded at 4.8 K with a magnetic field of 400 Oe applied perpendicular to the foil. The flux penetration is seen to advance in ridge-like structures, where each ridge has the characteristics of the

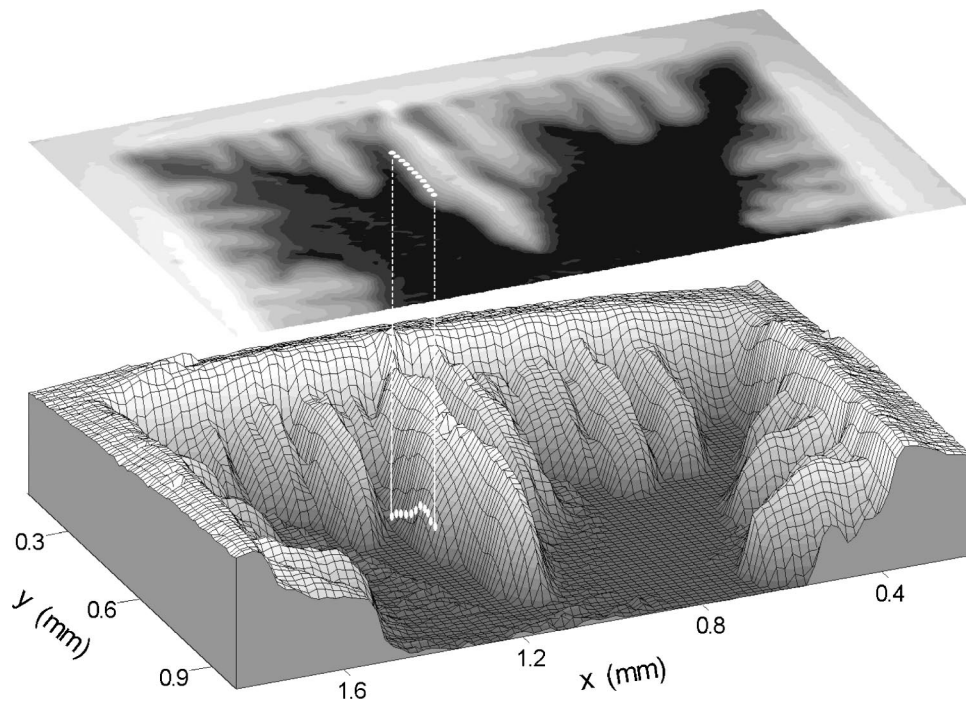


FIG. 1. Magnetic landscape of the Nb superconductor. The magneto-optical image (top) shows how the flux penetrates into one-half of a  $1.5 \times 1.5 \times 0.25$  mm<sup>3</sup> Nb foil at a field of 400 Oe applied perpendicular to the sample at  $T=4.8$  K. The image brightness represents the local density of the magnetic vortices. The 3D plot (bottom) of the penetration pattern shows that the magnetic landscape consists of several ridges with smooth slopes, which rise up from the flat Meissner state (flux free) area. Included in the figure is the location of a Hall probe array where each of the 11 probes detects the flux under an area of  $10 \times 10$   $\mu\text{m}^2$ . As the applied magnetic field increases all the ridges grow gradually on a macroscopic scale, quite similarly to the way sandpiles increase in size when grains are added.

critical state with an “inverted V” flux density profile (the MO investigation also showed that the ridge structure grows smoothly as the field is increased, and should not be confused with the dendritic structures abruptly appearing during thermal runaways in thin films<sup>15–17</sup>). In order to examine the local vortex dynamics within the magnetic landscape, several arrays of 11 Hall probes each were mounted at different spots of the sample, as shown in Fig. 2. The arrays were labeled I, II, III, IV, and V.

Figure 3 shows typical data obtained from one of the Hall sensors in array *I*, while a magnetic field perpendicular to the Nb foil was ramped from 0 to 3.5 kOe at the rate of  $1 \text{ Oe/s} \pm 0.05 \text{ Oe/s}$  using a superconducting magnet. Near 400 Oe the main curve makes an upturn, which indicates when the propagating flux front reached the probe position. Above 1 kOe the Hall signal grows linearly, corresponding to the Nb foil being fully penetrated. The whole curve follows the prediction of the critical state model for perpendicular geometries.<sup>18</sup> The resolution of the micro-Hall probe, which is made from a GaAl/AlGaAs heterostructure, is better than 0.21 G, equivalent to one flux quantum ( $\Phi_0 = 2.1 \times 10^{-15} \text{ T m}^2$ ) under the probe area. We quantify the Hall signal by the amount of flux associated with the vortices located under the  $10 \times 10 \mu\text{m}^2$  sensor area, and express it in number of flux quanta. Note that vortex movements producing flux variations smaller than  $\Phi_0$  can occur in the sample area under a given Hall probe, and their detection is only limited by our instrumental resolution. Although the overall curve appears smooth, the magnified views in the insets

clearly show that the amount of flux in a given area varies in distinct steps. This is direct evidence that the vortex penetration evolves by an avalanche-type of dynamics. As in previous micro-Hall probe studies, we measure an avalanche as the vertical size of the individual events. In our case, they ranged from fractions of a flux quantum to more than a hundred vortices. It should be noted that the definition of avalanche size used here is different from the usual definition

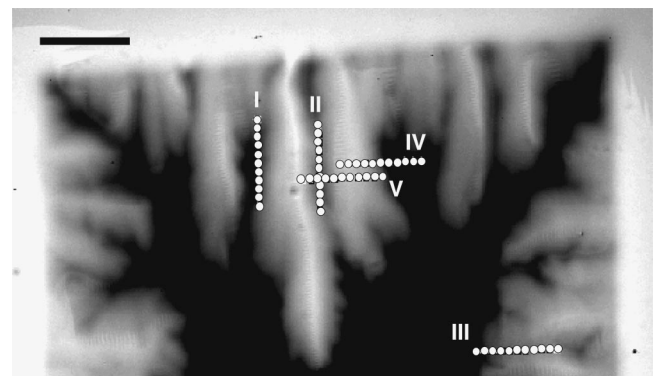


FIG. 2. Magneto-optical image of the sample with an overlay showing five different locations of the Hall probe array used for supplementary measurements. The image was taken at 450 Oe and 4.8 K, and the scale bar is 0.2 mm long. Location (I) is identical to the one in Fig. 1, and provided the data plotted in Fig. 3. The first four probes, counting from the left in location (IV), provided the data plotted in the inset of Fig. 4.

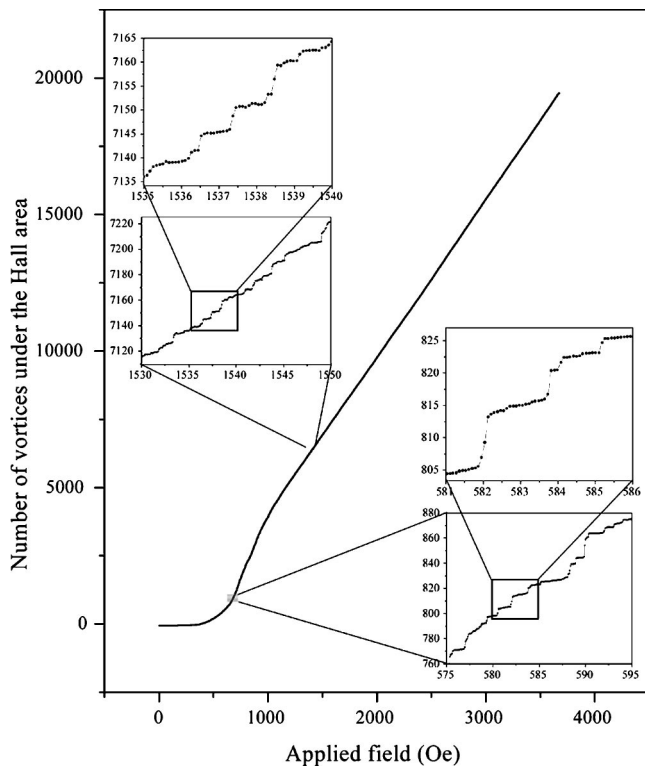


FIG. 3. Vortex avalanches seen by a Hall probe during field increase. The main curve was obtained from probe number 4 from the sample edge in Fig. 1, and contains more than 40 000 data points. The insets show zooms in two different field windows revealing distinct steps as a manifestation of avalanche dynamics. The experiment was performed at  $T=4.8$  K. Similar measurements performed slightly above  $T_c$  show no measurable steps, demonstrating that those reported in the figure are not mere instrumental noise.

used in theoretical “sandpile” models. In the models, such as the Bassler-Paczuski (BP) model for vortex dynamics,<sup>19</sup> avalanche size is defined as the number of lattice sites that “topple,” or equivalently, the number of vortex movements of unit length, during the course of an avalanche. Here the avalanche size is instead defined as the change in the number of vortices in a local area (the area covered by the Hall probe). However, the distribution of avalanche sizes defined using the alternative definition is also power law distributed for SOC sandpile models.<sup>20</sup> Thus either definition can be used to distinguish SOC behavior.

The overall flux dynamics can be viewed as a stepwise penetration of entire sections of the vortex lattice constituting the critical statelike ridges visualized in the MO pictures, in parallel with local reorganizations of the vortex distribution, which are detected with great accuracy by the Hall probes. Note that while the overall features of the flux penetration landscape were reproduced as the experiment was repeated under the same conditions, the detailed avalanche dynamics associated with the local vortex reorganizations did not, demonstrating an underlying complex dynamics. In principle, thermal fluctuations should also play a role, but the temporal output of a given Hall probe at a fixed external field showed to be stable, suggesting that thermal effects can be neglected in our case.

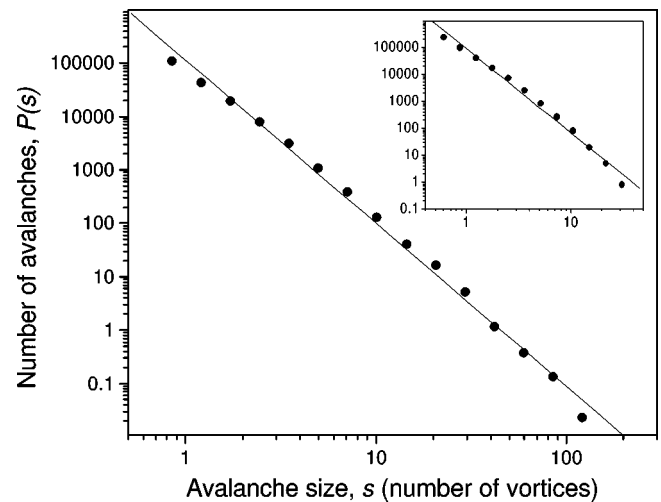


FIG. 4. Size distribution of avalanches. The statistics is based on nearly 200 000 avalanche events measured in the Hall probes located as shown in Fig. 1. Steps less than  $0.7\Phi_0$  were excluded from the counting of events.  $P(s)$  was averaged within exponentially increasing intervals along the  $s$  axis, giving equidistant points in the log-log plot. The data are fitted by the straight line  $P(s) \sim s^{-\tau}$ , with  $\tau=3.1 \pm 0.2$ . The inset shows analogous results using data from a very different Hall probe location (see Fig. 2), giving  $\tau=3.1 \pm 0.2$ .

In order to explore the statistical features of the avalanche dynamics at different regions of the sample, we combined the data from probes located in well-defined regions of the magnetic landscape (such as a “valley” between two ridges). This approach has two advantages. Firstly, instead of reporting highly local avalanche events using the output of a single probe, we can study the statistics of a wider region of the magnetic landscape without losing the high flux resolution of the individual probes, which is closer to the original SOC formulation. Secondly, the combined data from several Hall probes allows us to improve the statistics of the resulting avalanche size distributions to unprecedented levels.

Following the philosophy described above, the signals recorded from all the 11 probes in array I were subjected to further statistical analysis. A histogram of the avalanche sizes, taken as the number of magnetic flux quanta in a distinct step, is shown in Fig. 4. The data include approximately 200 000 avalanche events observed during several field sweeps up to 3.5 kOe repeated under identical external conditions. The number of avalanches,  $P(s)$ , versus their size is seen to behave as a power law over two and a half orders of magnitude in avalanche size  $s$ , with a critical exponent of  $\tau = 3.0 \pm 0.2$ . Note that our total number of avalanche events is about 100 times larger than in previous studies using micro-Hall probes,<sup>10–12,14</sup> and our distribution function spans more than six decades, which is essential for establishing a power-law distribution in this type of system. The plot in the inset corresponds to an analogous output from the first four probes counting from the left in array IV, and gives a critical exponent  $\tau=3.1 \pm 0.2$ .

To address the question of robustness, we also use outputs from arrays II, III, and V. From Fig. 2, where the different probe locations are indicated, one sees, e.g., that while all probes in array II are parallel to the same central ridge as



arrangement I, also avalanches coming from the neighboring “hillside” will contribute. All probes in array III are located parallel to two “competing” ridges, which, due to some degree of anisotropy in the sample, are thicker than those developing from the upper sample edge. A very different location is the one corresponding to the first four Hall probes on array IV, or to probes 5, 6, 7, and 8 on arrangement V (counting from the left). There, we are measuring “on top of the hill” avalanches. A remarkable result is that the avalanche size statistics performed on each of the above-mentioned groups of probes gave, in every case, quite good power laws over nearly one and a half decades on the horizontal axis, with critical exponent  $\tau$  consistent with the values reported above. This was also true for avalanche statistics from individual probes if enough events were collected after many runs.

As stated before, the existence of robust power laws in the avalanche size distribution is a distinctive feature of SOC. However, while the avalanche distribution is universal in SOC models (see, for example, Ref. 18), the slope of the flux density is not. Instead, it varies with the system parameters such as the local density, or strength, of pins. The topography we observe in Fig. 1 is reproducible from run to run, and hence the deviations we observe from a uniform penetration are due to quenched disorder. Nevertheless, the value of the

critical exponent  $\tau$  we measure is the same at all points in the sample, even though the local magnetic topography in the region of the probe varies from point to point. The fact that the exponents found in the present work are all essentially the same is characteristic of the universality expected for SOC. However, the high values of  $\tau$  found in our experiments can be better predicted by the ADCN theory, but that theory neglects the interaction between the components of the system. We believe that this assumption is quite unphysical in our case, and therefore that a modified SOC theory is more likely to best describe our results.

We appreciate the discussions with P. Bak, A. J. Batista-Leyva, H. Jaeger, B. Lorenz, R. Mulet, M. Paczuski, D. V. Shantsev, A. Malthe-Sørensen, and Y. Xue. The authors thank the support by the World Laboratory Center for Pan-American Collaboration in Science and Technology, the Research Council of Norway, the National Science Foundation, the Israel Science Foundation–Center of Excellence Program, the “Alma Mater” grants program (University of Havana), and the U.S. Department of Energy. The work in Houston was supported in part by the State of Texas through the Texas Center for Superconductivity and Advanced Materials at the University of Houston.

- 
- <sup>1</sup>P. Bak, *How Nature Works: The Science of Self-Organized Criticality* (Copernicus, New York, 1996).
- <sup>2</sup>H. Jensen, *Self Organized Criticality-emergent Complex Behavior in Physical and Biological Systems* (Cambridge University Press, Cambridge, 1998).
- <sup>3</sup>P. Bak, C. Tang, and K. Wiesenfeld, *Phys. Rev. Lett.* **59**, 381 (1987).
- <sup>4</sup>M. E. J. Newman and K. Sneppen, *Phys. Rev. E* **54**, 6226 (1996).
- <sup>5</sup>P. G. DeGennes, *Superconductivity of Metals and Alloys* (Benjamin, New York, 1966).
- <sup>6</sup>C. P. Bean, *Rev. Mod. Phys.* **36**, 31 (1964).
- <sup>7</sup>C. Tang, *Physica A* **154**, 315 (1993).
- <sup>8</sup>S. Field, J. Witt, F. Nori, and X. S. Ling, *Phys. Rev. Lett.* **74**, 1206 (1995).
- <sup>9</sup>C. Heiden and G. I. Rochlin, *Phys. Rev. Lett.* **21**, 691 (1968).
- <sup>10</sup>G. T. Seidler, C. S. Carrillo, T. F. Rosenbaum, U. Welp, G. W. Crabtree, and V. M. Vinokur, *Phys. Rev. Lett.* **70**, 2814 (1993).
- <sup>11</sup>R. J. Zieve, T. F. Rosenbaum, H. M. Jaeger, G. T. Seidler, G. W. Crabtree, and U. Welp, *Phys. Rev. B* **53**, 11849 (1996).
- <sup>12</sup>E. R. Nowak, O. W. Taylor, L. Liu, H. M. Jaeger, and T. I. Selinder, *Phys. Rev. B* **55**, 11702 (1997).
- <sup>13</sup>P. Esquinazi, A. Setzer, D. Fuchs, Y. Kopelevich, E. Zeldov, and C. Assmann, *Phys. Rev. B* **60**, 12454 (1999).
- <sup>14</sup>K. Behnia, C. Capan, D. Maily, and B. Etienne, *Phys. Rev. B* **61**, R3815 (2000).
- <sup>15</sup>C. A. Durán, P. L. Gammel, R. E. Miller, and D. J. Bishop, *Phys. Rev. B* **52**, 75 (1995).
- <sup>16</sup>P. Leiderer, J. Boneberg, P. Brull, V. Bujok, and S. Herminghaus, *Phys. Rev. Lett.* **71**, 2646 (1993).
- <sup>17</sup>T. H. Johansen, M. Baziljevich, D. V. Shantsev, P. E. Goa, Y. M. Galperin, W. N. Kang, H. J. Kim, E. M. Choi, M. S. Kim, and S. I. Lee, *Europhys. Lett.* **14**, 599 (2002).
- <sup>18</sup>E. Zeldov, J. R. Clem, M. McElfresh, and M. Darwin, *Phys. Rev. B* **49**, 9802 (1994).
- <sup>19</sup>K. E. Bassler and M. Paczuski, *Phys. Rev. Lett.* **81**, 3761 (1998).
- <sup>20</sup>T. J. Vadakkan, C. Lee, and K. E. Bassler (unpublished).